Studies on effects of umbelliferon derivatives against periodontal bacteria ; antibiofilm, inhibition of quorum sensing and molecular docking analysis

Studies on effects of Umbelliferon derivatives against periodontal bacteria; antibiofilm, inhibition of quorum sensing and molecular docking analysis.

Adnan Amin *[a], Muhammad Hanif [b], Khizar Abbas [c] Muhammad Ramzan [a], Abdur Rasheed [a], Ali Zaman [d] and Luc Pieters [e]

[a] NPRL, Department of Pharmacognosy, Faculty of Pharmacy, Gomal University, D.I. Khan, Pakistan.
[b] GCBB, Gomal University, D.I. Khan, Pakistan.
[c] Department of Pharmacognosy, Faculty of Pharmacy, Bahauddin Zakaria University, Multan, Pakistan
[d] UVAS, Gomal University, D.I.Khan, Pakistan.
[e] Natural Products & Food Research and Analysis, Department of Pharmaceutical Sciences, University of Antwerp, Belgium.

*Corresponding author

Dr. Adnan Amin
NPRL, Department of Pharmacognosy
Faculty of Pharmacy, Gomal University,
D.I.Khan, 29050, Pakistan.
adnan.amin@gu.edu.pk

Abstract

Objective: Umbelliferon derivatives are exclusively found in plants of *Ferula spp*. that are commonly used in curing various health concerns related to oral cavity. Diabetic patient are especially effected with periodontitis and allied complications.

Method: We investigated various compounds isolated from *Ferula narthex* exudate against clinical strains obtained from diabetic patients with periodontitis. Further antibiofilm, antiquorum sensing and molecular docking studies and ADMET analysis were performed.

Results: The docking target included 2Q0J, 2UV0, 3QP5 and 3QP1. HYDE affinity assessment was performed for the first 30 top ranking docked conformations within these active sites. The binding free energy ΔG, FlexX docking score and the most favorable poses for all the compounds were determined. During *in vitro* analysis, feselol presented high inhibition of *Pseudomonas aeruginosa* (MIC 0.01mg/mL, MBC 0.02mg/mL). Similarly, Feselol presented significant inhibition against clinical strain *S. epidermidis* (MIC 0.087 mg/mL, MBC 0.174 mg/mL) and *S. aureus* (MIC 0.087 mg/mL, MBC 0.087 mg/mL) preceded by 10'-*R*-acetyl-karatavacinol against *S. epidermidis* (MIC 0.56 mg/mL, MBC 0.56 mg/mL) and *S. aureus* (MIC 0.28 mg/mL, MBC 0.28 mg/mL). During antibiofilm inhibition assay, 10' *R*-acetyl-karatavacinol showed significant inhibition (54% at a final concentration 0.45 mg/mL), whereas slight antiquorum sensing activity was recorded.

Conclusions: The umbelliferon derivatives have significant inhibition of clinical isolates and moderate antibiofilm potential.

Key words: Clinical strains; molecular docking; Periodontitis; *Ferula narthex*; antiquorum sensing

1. Introduction

In addition to persistent hyperglycemia, diabetic patients generally have numerous complications, including periodontitis, which is an inflammatory illness of supporting tissues of teeth. Certain specific microorganisms are considered responsible for the progression of this disease, and further an advanced destruction of the periodontal ligament and alveolar bone with periodontal pocket formation may occur [1].

Periodontitis is a multifarious infectious disease, which is a consequence of the interaction of diverse bacteria, mostly due to bacterial biofilms [2]. This bacterial biofilm formation is considered as a problematic health concern, responsible for antibiotic resistance, and it is a consequence of quorum sensing (QS, cell-cell signaling). Biofilm formation is a mutual group behavior that encompasses various bacterial populations entrenched on a self-produced extracellular matrix [3]. The mutual performance of bacteria (biofilm) is mainly executed by QS, which is a cell-cell communication mechanism that coordinates gene expression in reply to population cell density [4]. It has been well established that a change in biofilm life style of a bacterial population is directed by QS as the population density reaches a certain threshold level [5,6].

Dentistry is facing a great problem of antibiotic resistance that could be specifically due to emergent bacterial biofilms [7]. Various antibiotics, which are associated with side effects, are generally used against this problem [8]. Thus, a quest to look for new treatment options is obvious; and traditional medicinal plants provide a promising option in this regard. The *Ferula narthex* Boiss. (Apiaceae) exudate is frequently used by local healers for antibacterial and analgesic effects in the oral cavity [9]. The exudate of this plant is a rich source of umbelliferone derivatives, which have been reported to possess interesting antimicrobial properties [10]. Based on traditional claims regarding the use of *Ferula narthex* in the oral cavity, we investigated the antibiofilm and QS inhibitory properties of various umbelliferone derivatives isolated from the exudate.

2. Material and Methods

2.1. Chemicals and solvents

The strains including *Chromobacterium violaceum* (DSM 30191) and *Pseudomonas aeruginosa* (ATCC 15442) were purchased from the German collection of microorganisms (DSM) and cell cultures, and the American Type Culture Collection (ATCC), respectively whereas *Staphylococcus epidermidis and Staphylococcus aureus* were isolated from patients. The growth media for bacteria including Lauria Bertani (LB), Tryptic soya broth (TSB) and nutrient agar were purchased from Hi Media (India). The tested umbelliferon derivatives were 8'-*O*-acetyl-asacoumarin A (**1**), 10'-*R*-acetyl-karatavacinol (**2**), asacoumarin A (**3**), 10'-*R*-karatavacinol (**4**) and feselol (**5**) (Fig. 1). The isolation and identification of these test compounds was reported earlier [11].

2.1 Molecular Docking Studies

2.1.1 Ligand and protein structure preparation

For docking studies, the X-ray crystallographic structures of the transcriptional regulators LasR (2UV0), PqsE (2Q0J) [12] and quorum sensing regulators CviR (3QP5) and CviR' (3QP1) [13] were obtained from the Protein Data Bank. The 3D structures of compounds were built using MOE builder tool [14] and the energy was minimized by MMFF94x force field [15]. All structures of required proteins were energy minimized by Molecular Operating Environment [14].

2.1.2 Molecular Docking Studies and Visualization

For docking analysis, the software LeadIT (BioSolveIT GmbH, Germany) [16] was used. While preparing receptors for docking studies, spacing of the amino acid residues was kept at 12.0 Å. Once the compounds were docked inside the binding pocket, the visual and binding affinities were assessed by HYDE (HYdrogen bonds and Dehydration) to inspect the contributions to binding of ligands with proteins [17]. Afterwards, visualization of the docked pose within the protein was carried out by Discovery Studio Visualizer (2017).

2.1.4 ADMET analysis

The ADMET analysis was performed using online tools including the SWISS ADME and pkCSM ADMET predictor.

2.3 Bacterial Isolation and sequencing

The ethical approval for the project was obtained (Ethical review Board, Gomal University, D.I.Khan, 2019). The dental plaques were collected from female diabetic patients after informed consent with the help of dentist. The Plaques were further processed for growth of bacteria using nutrient media. The isolation and purification of bacteria was performed using congo red agar. Finally the strains were submitted to National Culture collection of Pakistan (NCCP) to facilitate the 16S rRNA gene sequencing.

2.3.1 DNA Extraction and 16S rDNA Sequencing

The Genomic DNA from bacterial cultures was extracted using modified method [18] (Supplementary data file). This was followed by agarose gel electrophoresis and polymerase chain reaction (PCR) [19] (Supplementary data file). Finally, genes were aligned to the matching sequences available in the NCBI nucleotide database by nBLAST (Supplementary data Table 2).

2.4 Biological activities

2.4.1 Determination of MIC and MBC (minimum inhibitory and bactericidal concentrations)

The isolated compounds were assessed for antimicrobial activities using modified method [20] with slight modifications. In the MIC assay, the 96 microwell plates were loaded with 50 µL of the overnight-grown bacterial strain *Pseudomonas auruginosa* (ATCC 15442) (1.5×10^7 CFU/mL), followed by addition of 50 µL of test sample (various dilutions). The plates were incubated at 37 °C for 24 h. On the next day, 40 µL of resazurin solution (0.015 %) was added to each well followed by incubation at 37 a °C for further 60 min. Colorimetric readings were recorded using 96-microplate reader (Hippo MPP-96, Biosan). For MBC values, bacterial suspensions (10 µL) from the MIC microwells were relocated to already prepared agar plates

(Muller Hinton) and incubated for 24 h. Afterwards, bacterial growth was recorded on the agar plates. All samples were loaded in triplicate. Ciprofloxacin was used as positive control.

2.4.2 Antibiofilm Activity

The biofilm formation assay was performed using 12-well polystyrene plates with a slightly modified method [21]. Briefly, the bacterial strain (*P. auruginosa* ATCC 15442) was inoculated in TSB medium (280 µL) at an initial turbidity of 0.5 at 600 nm (0.5 McFarland). And allowed to incubate for 24 hrs to produce biofilm. Afterwards 100 µL of test compound (0.01-3 mg/mL) was added to the bacterial culture followed by incubation at 37 °C for further 24 h. Cell growth in the plates was measured at 592 nm. For quantification, the biofilms in the 12-well plates were stained using crystal violet. Afterwards 95% ethanol was added to the stained cells and absorbance was recorded at 592 nm to quantify total biofilm formation.

The % inhibition was calculated using following formula

$$\% \text{ inhibition} = (1 - \text{Abs of sample}/\text{Abs of control} \times 100)$$

2.4.3 Antiquorum sensing

The quorum sensing inhibition potential of isolated compounds was evaluated by a standard procedure [22] with slight modifications. An overnight culture of *C. violaceum* (1/100 ratio) was streaked onto LB agar in Petri dishes. Sterilized filter paper discs (6 mm) were prepared and placed on the top of BHIA (Brain Heart Infusion agar) seeded with indicator strain (*C. violaceum*). Then 15µL test compound (0.01-3 mg/mL) was applied on each disc and allowed to dry for 30 min. Afterwards, the assay plates were incubated at 30 °C for 3 days. Ciprofloxacin was used as standard drug. Finally, results were recorded by measuring the zone of inhibition around each disc.

2.4.4 Violacin inhibition assay

A modified method [23] was adopted for violacein inhibition assay. A 24 hrs old culture (200 µL of *C. violaceum* (OD= 0.4 OD at 600 nm) was loaded to sterilized microtiter plates

containing various concentrations of compounds (1-4 mg/mL). The plates were incubated at 30°C for 24 h and witnessed for the decrease in violacin pigment production by taking absorbance at 585 nm. The percentage inhibition was calculated by following the formula:

Violacein inhibition % = (1- Absorbance of Control /Absorbance of sample x 100)

Anti Swarming assay

3.0 Results and Discussions

3.1 Molecular Docking Studies

Molecular docking studies of test compounds was carried out in the active pocket of transcriptional regulators LasR (2UV0) and PqsE (2Q0J); and quorum sensing regulators CviR (3QP5) and CviR' (3QP1). All the compounds bind inside the pocket of these regulators, except asacoumarin A, although the related compound feselol binds inside both the receptors. However, the reason for inactivity may be the presence of an additional oxygen group at carbon 6 in asacoumarin A. The transcriptional regulator LasR is present in homo-tetramer form (chain E, F, G and H), and for docking chain E was selected based on earlier reports. The binding interactions between the test compounds and amino acid residues inside the active site of transcriptional regulator LasR, 2UV0 were visualized by Discovery Studio and LeadIT. The results are presented in the form of 3D and 2D molecular interactions. The amino acids involved in the active pocket are Tyr56, Ser129, Asp73, Trp60, Tyr64, Val76, Tyr47 and Ala50. The molecular docking studies demonstrated that the compounds fit in near vicinity to the active pocket of the regulator; however, notable interactions are shown by the test compounds with amino acids Pro41, Phe167, Lys16, Phe51, Gly54, Arg61, Ile52, Asn49, Tyr47, Gly123, Asp43, Glu124, Thr80, Phe167, Ala50, Asp65 and Ala58. The binding activity and the mode of interaction of the atoms in each molecule is shown in the 3D binding modes (Figure 2) and 2D representation (Figure S1). The cognate ligand, *N*-3-oxo-dodecanoyl-L-homoserine lactone, after docking in the protein pocket, showed the same interactions as presented earlier [24]. The transcriptional

regulator PqsE is present in a homo dimer form (chain A and B), and for docking chain A was selected based on earlier reports. When the binding modes of the test compounds inside the transcriptional regulator PqsE are monitored, amino acids residues Leu277 and Leu193 show favorable interactions with cognate ligand benzoic acid as well as test compounds. The most notable interactions shown by compounds **2**, **4** and **5** were with amino acid Arg108 (Figure 3 and Figure S2).

The compounds were also docked inside the active pocket of quorum sensing regulator CviR (3QP5). This protein exists as a homo tetramer form (A, B, C and D) and chain A was chosen for docking studies based on earlier reports. It was found that Trp84, Tyr88, Asp97, Leu100, Leu57, Asp97, Met135, Asn77 and Tyr80 were active site residues taking part in the formation of different interactions with the test compounds. The cognate ligand 4-(4-chlorophenoxy)-*N*-[(3S)-2-oxotetrahydrofuran-3-yl] was docked within the binding pocket and similar interactions were examined as reported earlier [13]. The compounds exhibited similar interactions as shown by the cognate ligand, except asacoumarin A, which was unable to bind inside the active pocket of 3QP5. Various important interactions were noticed by test compounds inside the binding site like hydrogen bonding, pi-pi interactions and pi-pi T shaped interactions. The binding activity of the atoms in each molecule is presented in the 3D poses (Figure 4) and 2D representation (Figure S3) within the active pocket of 3QP5.

When the binding arrangements of CviR' (3QP1) were noticed, the residues Ser155, Leu57, Val75, Tyr88, Tyr80, Leu100, Met135, Asp97, Trp84, Leu85, Glu54, Ser53, Leu72 and Arg159 were found to be involved in recognition of the active pocket. The cognate ligand of 3QP1 (*N*-[(3S)-2-oxotetrahydrofuran-3-yl] hexanamide) showed similar interactions as reported previously [13]. All the docked compounds occupied well the binding pocket and presented several important interactions. The 3D and 2D interaction diagrams of all the compounds are given in Figure 5 and Figure S4.

3.2 HYDE assessment of compounds against all the targets

The HYDE affinity assessment was done for the first 30 top ranking docked conformations within the active sites of 2Q0J, 2UV0, 3QP5 and 3QP1. The results were helpful during

assortment of the correct binding mode. The binding free energy ΔG, FlexX docking score and the most favorable poses for all the compounds are given in Table 1. The compounds bind to the receptor with specific binding affinity and give encouraging contributions.

3.3 ADMET analysis

The ADMET properties of all compounds are shown in Table 1. The feature TPSA is related to the absorption properties of compounds, whereras Consensus Log $P_{o/w}$ is indicator for lipophilicity. It was evident that TPSA topological polar surface area was less than 100 that indicates good oral absorption or membrane permeability [25-26]. Like wise the compounds presented poor lipophilicity [27]. The detailed analysis of ADMET are shown in Table 2.

3.4 *In vitro* analysis

The compounds were initially analyzed for determination of MIC and MBC against biofilm producer strain *Pseudomonas aeruginosa* (ATCC 15442). Among all, compound **5** presented notable activity (MIC 0.01 mg/mL, MBC 0.04 mg/mL) followed by **4** (MIC 1.2 mg/mL, MBC 2.4 mg/mL) (Table 2) whereas **3** was recorded as inactive (MIC >3 mg/mL). The isolated compounds were further tested for the antibiofilm potential against the biofilm producing strain *P. aeruginosa* (ATCC 15442). Amongst all analyzed compounds, **2** showed high activity (54% inhibition at a final concentration 0.45mg/mL), whereas compound **4** presented notable inhibition of biofilm formation (55%) at a higher concentration (final concentration 3 mg/mL) (Table 2). These results are consistent with the *in silico* analysis that indicated a strong interaction of **2**, **4** and **5** were with amino acid Arg108 (Table 3).

Further the compounds were tested against clinical strains of *S. epidermidis* and *S. aureus.* The compound **5** presented significantly high activity against *S. epidermidis* (MIC 0.087 mg/mL, MBC 0.174 mg/mL) and *S. aureus* (MIC 0.087 mg/mL, MBC 0.087 mg/mL). Likewise, compound **2** presented nicer inhibition against tested strains *S. epidermidis* (MIC 0.56 mg/mL, MBC 0.56 mg/mL) and *S. aureus* (MIC 0.28 mg/mL, MBC 0.28 mg/mL). All other compounds were active, however inhibition was at higher concentrations (Table 5), that shows higher resistance levels.

On the other hand, during anti-quorum sensing evaluation, none of the compounds showed activity at the tested concentrations (final concentration 3 mg/mL). Likewise a week inhibition of violacein inhibition was recorded (Table 5). Upon comparison with *in silico* analysis, it was noticed that all compounds except asacoumarin A showed binding inside the pocket of the regulators, whereas asacoumarin A showed a fit in the near locality of the active pocket. Subsequently, the acetyl derivative i.e compound **3** also presented no activity (Table 4) that could be due to similar structural features (Figure 1). Thus, the *in vitro* and *in silico* results are in close correspondence with each other.

It was concluded that *Ferula narthex* compounds possess significant inhibition of clinical isolates and moderate antibiofilm potential with no antiquorum sensing activity.

Acknowledgment

The Foundation "Plants for Health" is kindly acknowledged for financial support to Dr. Adnan Amin

Conflict of interest

The authors declare no conflict of interest

References

[1] M.G.Newman, F.A. Carranza, H. Takei, P.R. Klokkevold. Carranzas clinical Periodontology. 10th ed. (2006) Elsevier health sciences.

[2] P. D. Marsh. Dental plaque as a biofilm and microbial community-implication for health and diseases. BMC Oral Health. 6(2006) S14. d.

[3] C. Solano, M. Echerverch, I. Lasa. Biofilm dispersion and quorum sensing. Curr. Opin. Microbiol. 18 (2014) 96-104. doi: 10.1016/j.mib.2014.02.008.

[4] C.D. Nadell, J.B Xavier, S.A Levin, K.R. Foster. The Evolution of Quorum Sensing in Bacterial Biofilms. PLOS. Biol. 6 (2008):e14.

[5] M.E. Davey, G.A O'Toole Microbial biofilms: from ecology to molecular genetics. Microbiol. Mol. Biol. Rev. 64(2000) 847–867.

[6] B. Hammer, B. Bassler Quorum sensing controls biofilm formation in *Vibrio cholerae*. Mol. Microbiol. 50(2003) 101–104.

[7] M. Wróblewska, I. Strużycka, E. Mierzwińska-Nastalska. Significance of biofilms in dentistry. Przegl Epidemiol. 69(2015), 879-83.

[8] V. D'Argenio, F. Salvatore The role of the gut microbiome in the healthy adult status. Clin. Chim. Acta. 7 (2015) 97-102.

[9] P. Mahendra, S Bisht . *Ferula asafoetida*: Traditional uses and pharmacological activity. Pharmacogn Rev.6(2012):141-6. doi: 10.4103/0973-7847.99948.

[10] L. Yang, W. Ding., Y Xu, , D Wu. ., S Li,., S Chen,., B Gou,. 2016. New Insights intothe Antibacterial Activity of Hydroxycoumarins against *Ralstonia solanacearum. Molecules*, 21(2016), 468
https://doi.org/10.3390/molecules21040468.

[11] A. Amin, E. Tuenter, P Cos, L Maese, V. Exarchou, S. Apers, L. Pieters. Antiprotozoal and Antiglycation Activities of Sesquiterpene Coumarins from *Ferula narthex* Exudate Molecules 21(2016) 1287; doi:10.3390/molecules21101287.

[12] S Yu, V. Jensen, J. Seeliger, I. Feldmann, S. Weber, E. Schleicher, et al. Structure elucidation and preliminary assessment of hydrolase activity of PqsE,

the *Pseudomonas* quinolone signal (PQS) response protein. Biochemistry-US 48, (2009) 10298-307.

[13] G. Chen, L. R Swem, D.L. Swem, D.L. Stauff, C.T. O'Loughlin, P.D. Jeffrey, B.L. Bassler, F.M. Hughson. A Strategy for Antagonizing Quorum Sensing. Mol. Cell. 42(2011) 199-209.

[14] MOE (Molecular Operating Environment) Version 2016.01. Chemical Computing Group, (CCG).
http://www.chemcomp.com/MOE Molecular_Operating_Environment.htm.

[15] P. Labute, Protonate 3D: Assignment of ionization states and hydrogen coordinates to macromolecular structures Proteins.75(2009): 187–205

[16] LeadIT version 2.3.2; BioSolveIT GmbH, Sankt Augustin, Germany, 2017, www.biosolveit.de/LeadIT.

[17] N. Schneider, G. Lange, S. Hindle, R. Klein, M. A. Rarey Comput. Aided Mol. Des. 27(2013)15-29.

[18] D.G. Pitcher, N. A. Saunders, R. J. Owen. Rapid extraction of bacterial genomic DNA with guanidium thiocyanate. Lettr. Appl. Microbiol. 8(1989)151-156.

[19] M. Joshi, J.D. Deshpande. Polymerase chain reaction: methods, principles an application. Int. J. Biomed. Res. 2(2010) 81-97.

[20] A. H.K Weseler, R. Geiss, J. Saller, A. Retching. A novel colorimetric broth microdilution method to determine the minimum inhibitory concentration (MIC) of antibiotics and essential oils against Helicobacter pylori. Pharmazie. 60(2005) 498–502.

[21] M.M., Bazargani, J. Rohloff. Antibiofilm activity of essential oils and plant extracts against Staphylococcus aureus and Escherichia coli biofilms. Food Control. 61(2016) 156-164.

[22] K.M. Koh, F.Y. Tham. Screening of traditional Chinese medicinal plants for quorum-sensing inhibitors activity. J. Microbiol. Immunol. Infect. 44 (2011): 144–148

[23] R.J.C. McLean, L.S. Pierson III, C. Fuqua. A simple screening protocol for the identification of quorum signal antagonists. J. Microbiol. Methods 58(2004) 351–360.

[24] M. J. Bottomley, E. Muraglia, R. Bazzo, A. Carfi. Molecular insights into quorum sensing in the human pathogen *Pseudomonas aeruginosa* from the structure of the virulence regulator LasR bound to its autoinducer. J. Biol. Chem. 282(2007) 13592-600.

[25] P. Ertl , B. Rohde, P. Selzer. Fast Calculation of Molecular Polar Surface Area as a Sum of Fragment-Based Contributions and Its Application to the Prediction of Drug Transport Properties J. Med. Chem. 43, (2000), 3714-3717. doi.org/10.1021/jm000942e

[26] T. Qidwai, T. (2016). QSAR modeling, docking and ADMET studies for exploration of potential anti-malarial compounds against Plasmodium falciparum. In Silico Pharmacol. 5(2016) doi: 10.1007/s40203-017-0026-0.

[27] P. Fonteh, A. Elkhadir, B. Omondi, I. Guzei, J. Darkwa, D. Meyer, D. Impedance technology reveals correlations between cytotoxicity and lipophilicity of mono and bimetallic phosphine complexes. Biometals 28(2015), 653– 667. doi: 10.1007/s10534-015-9851-y.

[28] Y. Han, J. Zhang, C.Q. Hu, X. Zhang, B. Ma, P. Zhang. *In silico* ADME and Toxicity Prediction of Ceftazidime and Its Impurities. Front. Pharmacol. 10 (2019):434. doi: 10.3389/fphar.2019.00434.

Figure legends

Figure 1. Structures of isolated compounds from the *Ferula narthex* exudate.

Figure 2. 3D interactions of **a**) Compound **1** **b**) Compound **2 c**) Compound **3 d**) Compound **4 e**) Compound **5** and **f**) *N*-3-oxo-dodecanoyl-L-homoserine lactone inside the transcriptional regulator 2UV0.

Figure 4. 3D interactions of **a**) Compound **1 b**) Compound **2 c**) Compound **3 d**) Compound **4 e**) Compound **5** and **f**) 4-(4-chlorophenoxy)-*N*-[(3S)-2-oxotetrahydrofuran-3-yl]butanamide inside the pocket of quorum sensing regulators CviR (3QP5)

Figure 3. 3D interactions of **a**) Compound **1 b**) Compound **2 c**) Compound **3 d**) Compound **4 e**) Compound **5** and **f**) benzoic acid inside the pocket of transcriptional regulator 2Q0J.

Figure 5. 3D interactions of **a**) Compound **1 b**) Compound **2 c**) Compound **2 d**) Compound **3 e**) compound **5** and **f**) *N*-[(3S)-2-oxotetrahydrofuran-3-yl]hexanamide inside the pocket of quorum sensing regulators CviR' (3QP1).

Table Legends

Table 1. Docking and Hyde scores and their corresponding ranks by Hyde affinity assessment.

Table 2 ADMET properties of compounds

Table 3. MIC and MBC values of umbelliferon derivatives against *Pseudomonas aeruginosa*

Table 4. MIC and MBC values of umbelliferon derivatives against isolated bacterial strains.

Table 5. Inhibition of microbial biofilm and Quorum sensing and Violacine by umbelliferon derivatives.

LIST OF TABLES

Table 1.

Code	FlexX score of the top-ranking pose	Poser rank	Binding free energy ΔG (kJ mol^{-1})	H Bond Interaction Residues
2Q0J				
1	−14.29	1	−32	Asp 196, Leu 281, Ser 285, Phe 195, Leu 277, Tyr 72, Asp 73, His 71, fe 998
2	−17.33	3	−16	Tyr 72, Lys 70, Ser 285, His 71, Leu 193, Leu 277, His282, Ser 273
3	−10.96	2	−21	Val 108, Leu 112, Tyr 72, Lys 70, Arg 288, Phe 195, His 71
4	−11.84	1	−22	His 71, Tyr 72, Arg 288, Leu 112, Asp 196, Leu 193, Pha 195
5	−15.16	6	−10	His 71, Leu 277, Leu112, Tyr 72, Ser 160, Asp 161, Asp 196, Arg 198, Val 108,
2UV0				
1	−6.76	2	−9	Pro41, Phe167, Phe 51 Ile 52, Ala 50, Arg 61
2	−5.01	1	−15	Ala 50, Val 53, Arg 61 Ile 52
3	−10.27	3	−9	Tyr 47, Gly123, His 119, Leu 125, Asp 43,Thr 80
4	−9.99	2	−19	Ile 52, Ala 50, Phe 51, Arg 61, Val 53, Asn 49, Phe 167
5	−11.42	6	−15	Asn 49, Glu 48, Arg 67, Ala 68, Ile 52, Gly 54
3QP5				
1	-4.55	1	-13	Leu 57, Tyr 88, Trp 84, Met 89, Leu 85, Asn 77, Leu76
2	-10.31	3	-39	Leu 57, Val 75, Leu 72, Ile 153, Leu 100, Ile 99, Ser 155, Phe 126, Asp 97, Trp 34, Met 135, Trp111
3	-8.50	4	-12	Val 109, Glu 113, Arg 114, Pro96, Arg 101.

4	-10.79	8	-38	Leu 57, Val 75, Phe 126, Trp 34, Trp111, Asp97, Tyr 33, Leu 35, Asn 77
5	-10.10	9	-31	Met 135, Leu 57, Trp111, Asp97, Ile 97, Val 75,Trp 84, Tyr80, Leu 85, Leu 100, Leu 72
3QP1				
1	-7.02	2	-18	Thr 131, Gly 136, Ser 137, Arg 159, Gly 158, Ser 53, Gly 134, Ala 157, Arg 55, Gly 158, Glu 54
2	-7.52	1	-10	Ser 53, Glu 112, Ser137, Arg 159, Arg 55, Gly 136, Glu 54, Thr 131, Gly 153,
3	-9.83	6	-46	Tyr 88, Ile153, Leu 57, Leu 100, Met 89, Tyr 80, Val 75, Leu 85
4	-14.40	5	-20	Gly 134, Gly 136, Thr 131, Glu 54, Ala 157, Ser 137, Gly 153, Arg 55, Glu 112, Arg 159
5	-6.06	1	-13	Arg 101, Gln 70, Arg 71, Ile69, leu 100, Leu 72, Gln 5, Ala94

Table . 2

Properties	Compound				
	1	**2**	**3**	**4**	**5**
TPSA (A°)	85.97	85.90	79.90	79.90	59.67
Consensus Log $P_{o/w}$	4.800	4.89	4.38	4.50	4.40
Absorption					
Water solubility (logmol/L)	-5.753	-6.381	-4.56	-5.666	-5.328
$CaCo_2$ permeability (log Papp in 10^{-6} cm/s)	0.906	0.713	0.996	0.816	1.303
Intestinal absorption (human) (% absorbed)	94.267	94.402	93.954	93.257	93.713
Skin permeability (log Kp)	-3.08	-2.806	-3.079	-3.026	-2.967
P-Glycoprotein substrate	Yes	No	Yes	Yes	Yes
P-Glycoprotein I inhibitor	Yes	Yes	Yes	Yes	Yes
P-Glycoprotein II inhibitor	Yes	Yes	Yes	Yes	Yes
Distribution					
VDss (human, log L/kg)	0.141	0.211	0.321	0.13	0.554
Fraction unbound (human) (Fu)	0.077	0	0.125	0	0.057
BBB permeability(logBB)	-0.627	-0.822	-0.244	-0.582	-0.117
CNS permeability (log PS)	-2.315	-2.4	-2.349	-2.571	-1.702
Metabolism					
CYP2D6 substrate	No	No	No	No	No
CYP3A4 substrate	No	Yes	No	Yes	Yes
CYP1A2 inhibitor	No	No	No	No	Yes
CYP2C19 inhibitor	Yes	Yes	Yes	Yes	No
CYP2C9 inhibitor	Yes	Yes	Yes	Yes	No
CYP2D6 inhibitor	No	No	No	No	No
CYP3A4 inhibitor	Yes	Yes	Yes	Yes	No
Excretion					
Total clearance (logml/min/kg)	1.382	1.152	1.393	1.307	0.345
Renal OCT2 substrate	No	No	No	No	Yes
Toxicity					
AMES toxicity	No	No	No	No	No
hERG I inhibitor	No	No	No	No	No
hERG II inhibitor	Yes	Yes	Yes	Yes	Yes
Hepatotoxicity	No	No	Yes	Yes	No
Skin sensitization	No	No	No	No	No

ADMET, absorption, distribution, metabolism, excretion, and toxicity; TPSA topological polar surface area; Consensus Log $P_{o/w}$ average of five different lipophilicities; Papp, apparent permeability coefficient; AMES, assay of the ability of a chemical compound to induce mutations in DNA; Kp, skin permeability constant; Fu, fraction unbound; BBB, blood–brain barrier; BB, blood–brain; CNS, central nervous system; PS, permeability-surface area; T. pyriformis, Tetrahymena pyriformis; LD, lethal dose; LOAEL, lowest-observed-adverse-effect level. Adopted from [28]

Table 3.

Compound	MIC (mg/mL)	MBC (mg/mL)
1	2.65	2.65
2	1.12	1.12
3	>3	> 3
4	1.2	2.4
5	0.01	0.04
Positive control[1]	0.004	0.006

[1] Ciprofloxacin

Table 4.

Compound	*Staphylococcus epidermidis*		*Staphylococcus aureus*	
	MIC (mg/mL)	MBC (mg/mL)	MIC (mg/mL)	MBC (mg/mL)
1	2.23	2.23	2.23	>2.23
2	0.56	0.56	0.28	0.28
3	1.77	>3.54	3.54	>3.54
4	4.2	>4.2	2.1	>4.2
5	0.087	0.174	0.087	0.087
Ciprofloxacin*	5	5	5	5
Azithromycin*	20	20	20	20
Metronidazole*	156	312	156	156

* µg/mL

Table 5.

Compound	Antibiofilm (% inhibition)	Anti quorum sensing (mm)	% of violacein inhibition
1	2 [1]	1	2
2	54 [2]	0	0
3	15[1]	1	5
4	55[1]	0	0
5	Not tested	Not Tested	Not Tested
Standard	63 [3]	16 [4]	78

[1] highest final concentration 3 mg/ml, [2] at final concentration 0.45mg/ml, [3] Ciprofloxacin at 78µg/ml, [4] Ciprofloxacin at 30 µg/mL, **Noted tested** due to very low concentration.

LIST OF FIGURES AND TABLES

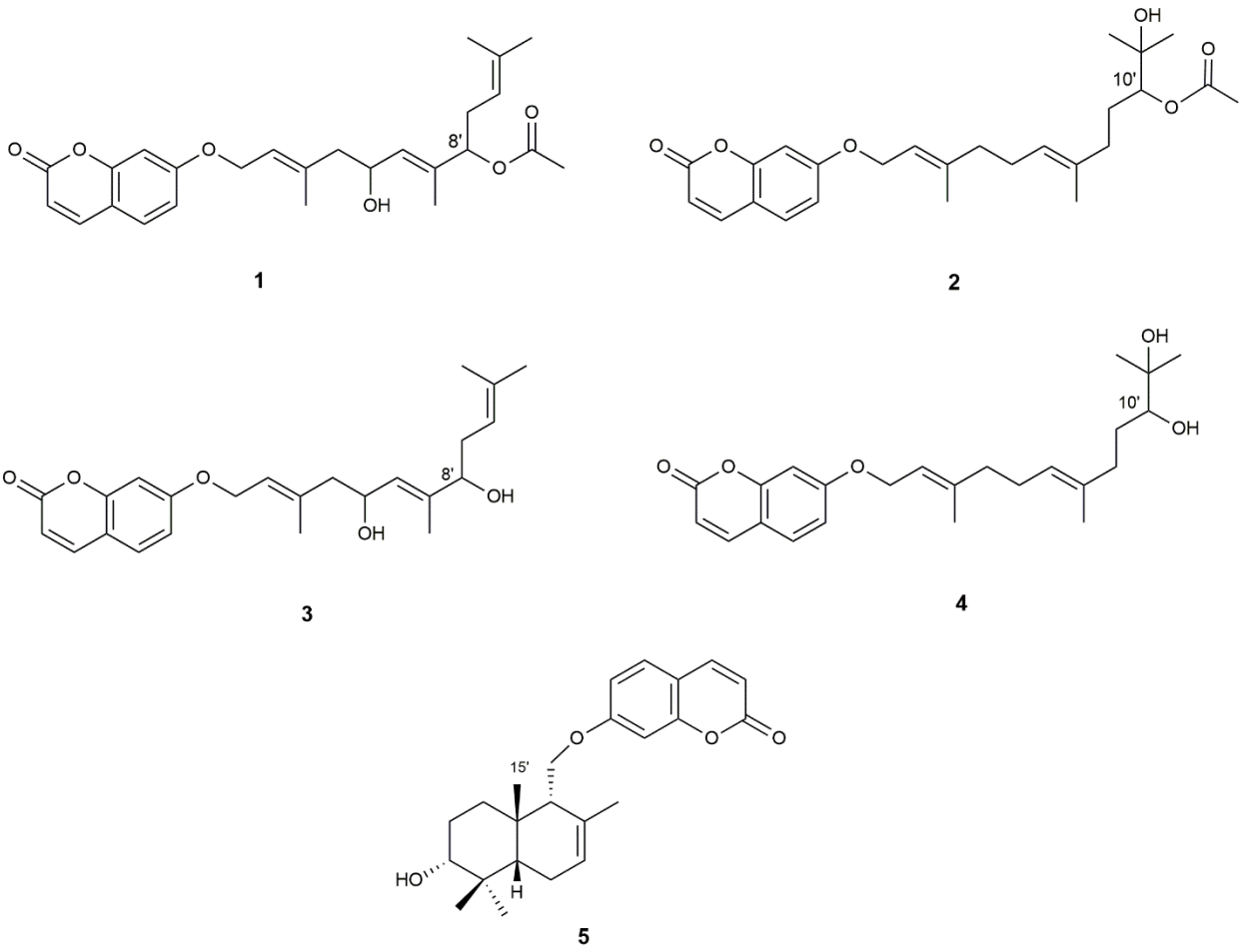

Figure 1.

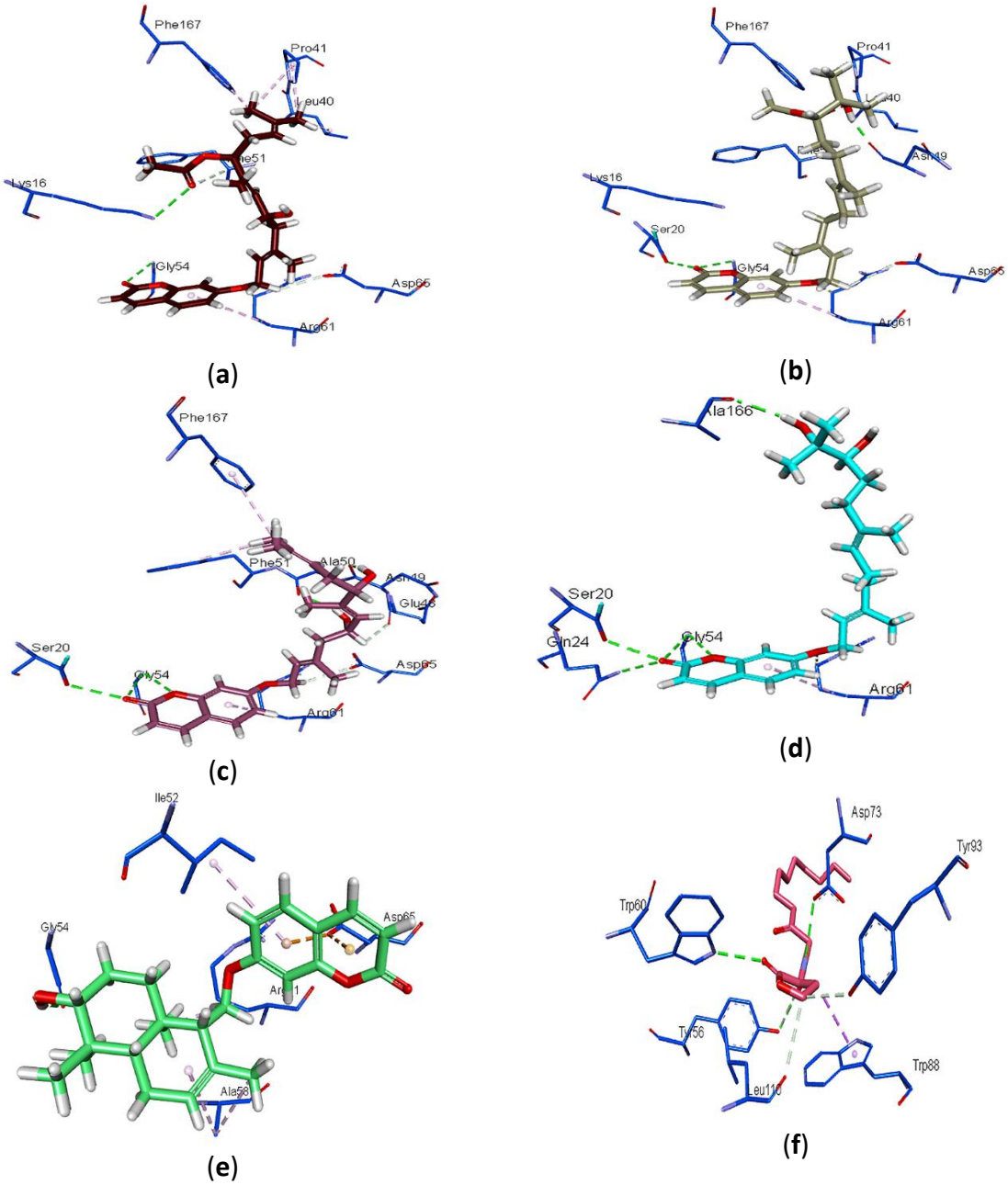
Phe167
Pro41
Leu40
Lys16
Gly54
Asp65
Arg61
(a)
Phe167
Pro41
Asn19
Lys16
Ser20
Gly54
Asp65
Arg61
(b)
Phe167
Phe51
Ala50
Asn19
Glu49
Ser20
Gly54
Asp65
Arg61
(c)
Ala166
Ser20
Gln24
Gly54
Arg61
(d)
Ile52
Gly54
Asp65
Ala58
(e)
Asp73
Tyr93
Trp60
Tyr56
Leu110
Trp88
(f)

Figure 2.

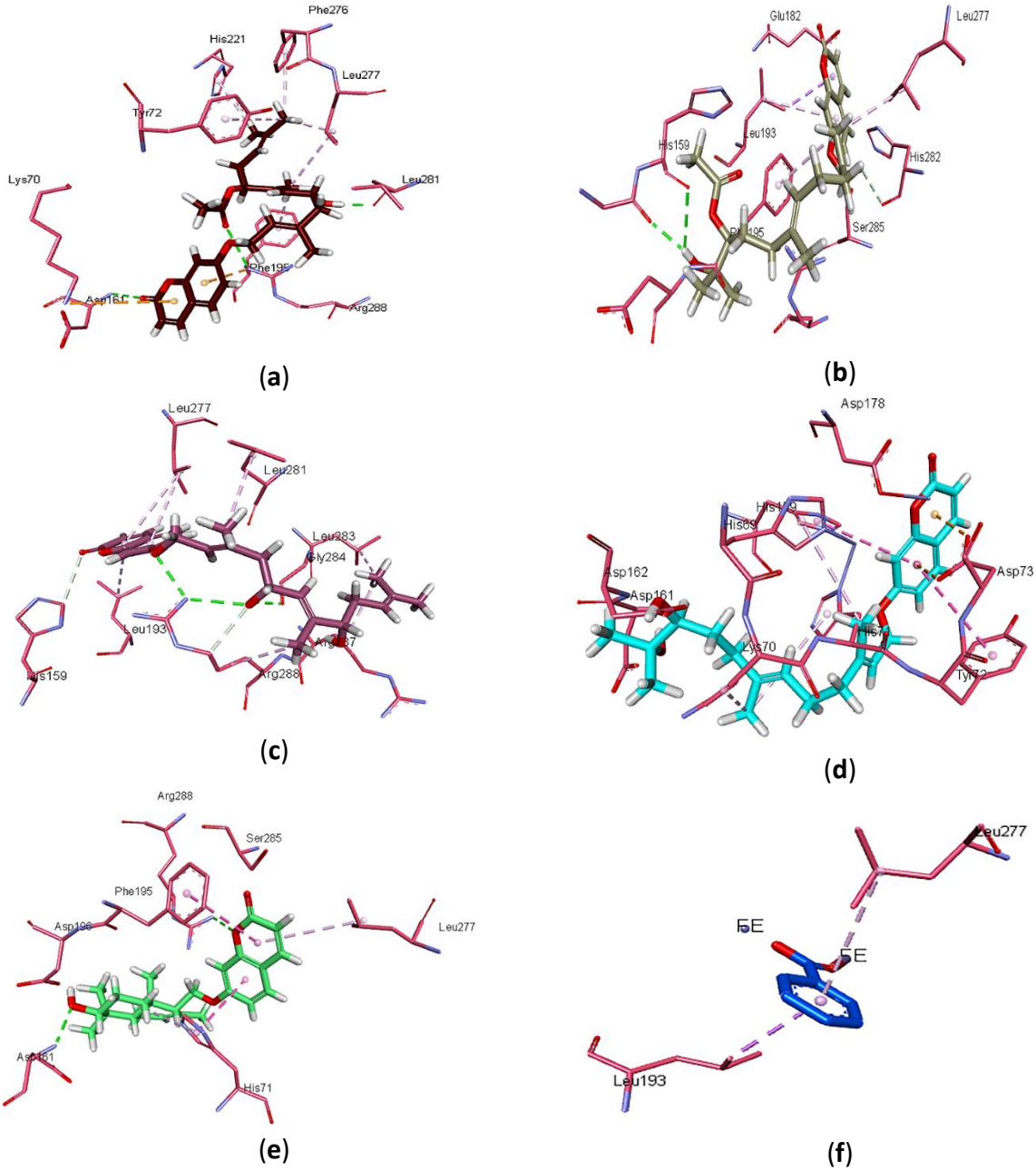
Phe276
His221
Leu277
Tyr72
Lys70
Leu281
Asp161
Phe195
Arg288
(a)
Glu182
Leu277
Leu193
His159
His282
Ser285
(b)
Leu277
Leu281
Leu283
Gly284
Leu193
His159
Arg288
(c)
Asp178
His69
Asp162
Asp161
Asp73
Lys70
Tyr72
(d)
Arg288
Ser285
Phe195
Leu277
His71
(e)
Leu277
Leu193
(f)

Figure 3.

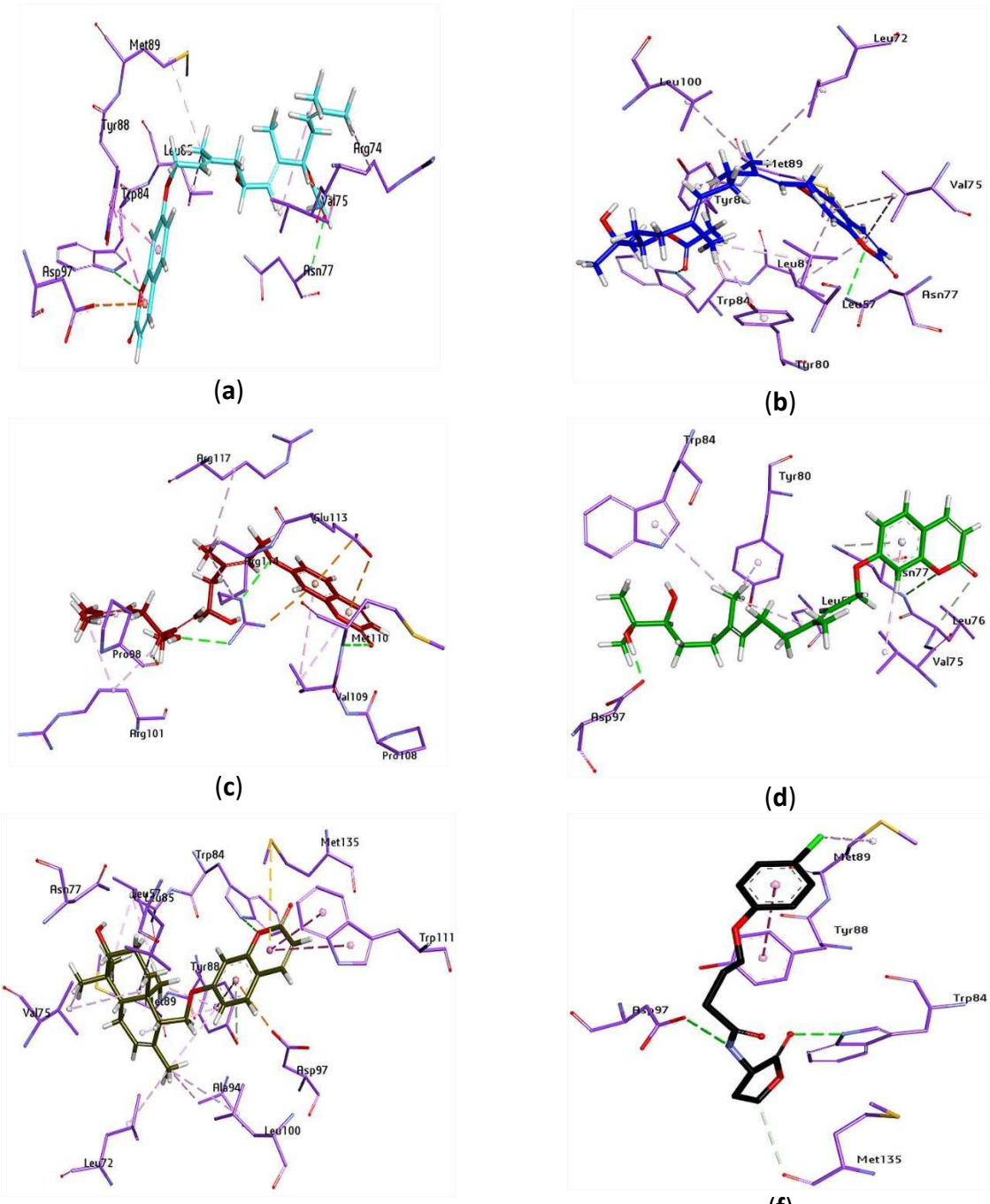
Met89
Tyr88
Arg74
Trp84
Val75
Asp97
Asn77
(a)
Leu72
Leu100
Met89
Val75
Trp84
Asn77
Tyr80
(b)
Arg117
Glu113
Met110
Pro98
Val109
Arg101
Pro108
(c)
Trp84
Tyr80
Asn77
Leu76
Val75
Asp97
(d)
Met135
Trp84
Asn77
Trp111
Tyr88
Val75
Asp97
Ala94
Leu100
Leu72
(e)
Met89
Tyr88
Trp84
Asp97
Met135
(f)

Figure 4.

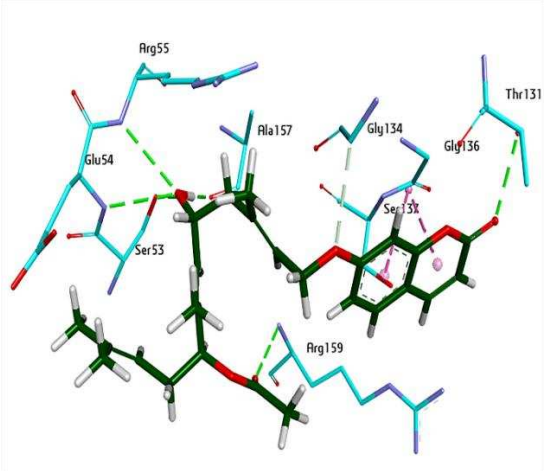

(a)

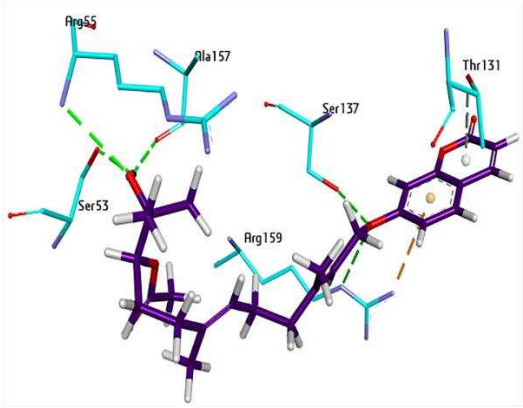

(b)

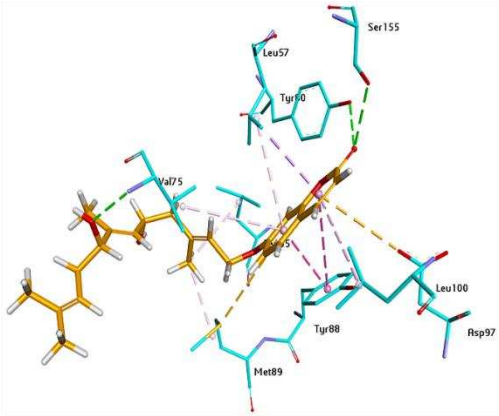

(c)

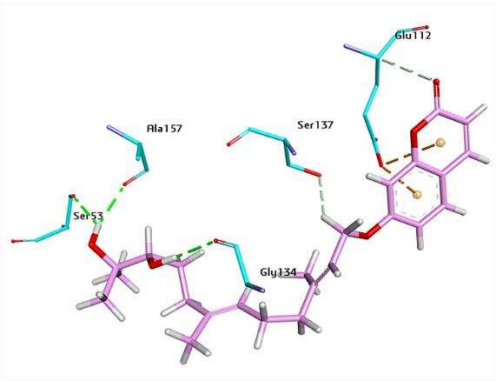

(d)

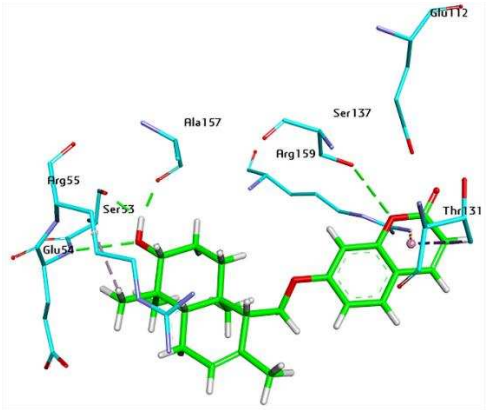

(e)

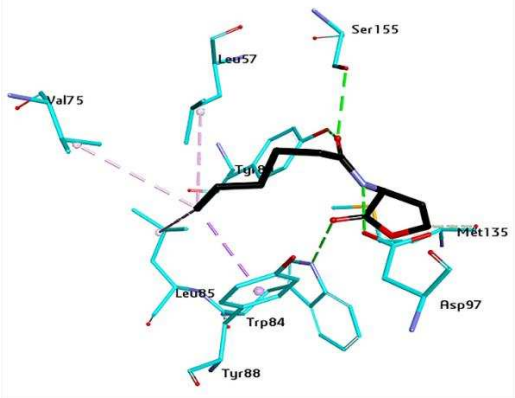

(f)

Figure 5.

Studies on effects of Umbelliferon derivatives against periodontal bacteria; antibiofilm, inhibition of quorum sensing and molecular docking analysis.

Supplementary data file

DNA Extraction and 16S rDNA Sequencing

Briefly the bacterial colonies were collected Muller Hinton agar plates and placed in lysis solution (500 µL) in microtubule and incubated for 20-30 minutes at room temperature. This was followed by centrifugation for 3 minutes at 13000 rpm for phase separation. The supernatant was discarded while the pellet containing DNA was further processed (multiple washings with lysis solution). Pellet was again treated with 400 µl lysis solution, 13 µl of 20% SDS (Sodium Dodecyl sulphate) and 25 µl proteinase K. Samples were incubated at 37°C overnight.

The samples were treated further with 500 µl of phenol, chloroform and isoamyl alcohol (i.e. PCI solution). The suspended solutions were centrifuged at 13000 rpm for 10 minutes for gentle and through mixing. Aqueous phase was transferred to other tube for purification and separation of DNA. The aqueous layer was treated with 500 µl of chloroform and isoamyl alcohol (C:I, 24:1) and centrifuged again for 10 minutes at 13000 rpm. The aqueous layer was shifted into 1.5 ml centrifuge tube, 55 µl of sodium acetate and 500 µl of chilled isopropanol were added. Samples were incubated for 45 minutes at -20°C. Samples were centrifuged at 13000 rpm for 10 minutes. Supernatant was discarded and pellet was treated with 500 µl of 70% ethanol and centrifuged at 7500 rpm for 5 minutes in order to remove all impurities, pellet was kept while supernatant was discarded and air dried. DNA pellet was resuspended in TE Buffer (Tris EDTA) and stored at 4°C.

Agarose Gel Electrophoresis:

Gel electrophoresis was performed using 1% agarose gel and the composition included 1 gram of agarose which was dissolved in 100 ml of 1X TAE buffer (Tris Acetic acid EDTA). Clear solution was formed after heating. 7 µl Ethidium Bromide was added in gel solution. Gel was poured into

the gel casting tray with inserting combs. After solidification, gel caster was transferred to gel

16SV3V4-F	CCTANGGGNNGCANCAG	
16SV3V4-R	GGACTACNNGGGTATCTAAT	TCCTCCGCTTATTGATATGC

tank filled with 1X TAE buffer and combs were removed carefully. 2 µl of extracted DNA was mixed with 2 µl of 6X bromophenol blue dye (loading dye) and it was loaded in wells. The gel was run under specific parameters which included 500 mA of current with 75 volts for 35 minutes. Gel was visualized under UV Trans-Illuminator bio Doc Analyzer. Following gel picture is showing representative DNA bands with comparison to 1KB Ladder:

Polymerase Chain Reaction (PCR):

PCR is a molecular biology technique used to amplify a single copy or a specific sequence of DNA. 16SV3V4 primers were used to amplify the fungal samples. Sequences of forward and reverse primers are:

Following chemicals at provided concentrations were used:

- Template DNA
- Forward & reverse Primer (BGI Company)
- Taq polymerse enzyme 5U/ µL (Solis BioDyne FIREPol DNA polymerase, 01-01-00500)
- PCR buffer (Solis BioDyne FIREPol DNA polymerase, 01-01-00500)
- $MgCl_2$ (Solis BioDyne FIREPol DNA polymerase, 01-01-00500)
- dNTPs (Solis BioDyne, dNTPs Set, 02-21-00400)
- PCR water (Invitrogen RT PCR garde water, AM9935)

PCR Reagents	**Stock Conc.**	**Working Conc.**	**Vol/Rec**	**Vol. x (n)**
DNA template	-	-	1 µL	
pF	10 µM	0.2 µM	0.4 µL	
Pr	10 µM	0.2 µM	0.4 µL	
DNTPs	10 mM	0.2 Mm	0.4 µL	
Buffer	10X	1X	2 µL	
$MgCl_2$	25 mM	2.5 Mm	2 µL	
taq Polymerase	5U/ µL	1.5 U	0.3 µL	

PCR H_2O		13.5 µL	
Final Volume		20 µL	

"n" would be any number for which you are making master mix.

Polymerase chain reactions were performed on a Galaxy XP Thermal Cycler (BIOER, PRC). Optimized PCR conditions were shown in table.

Table 1: Optimized PCR conditions

Steps	Sub-cycles	Conditions	PCR cycles
Initial Denaturation		95 °C, 10 min	1
PCR Cycles	Denaturation	95 °C, 1 min	40
	Primer annealing	54 °C, 1 min	
	Primer extension	72 °C, 1 min	
Final extension		72 °C, 10 min	1
Hold		04 °C, ∞	1

Table.2 Identification of strains based on 16S rRNA gene sequence published in DNA database.

S.No	Strain ID	Number of nucleotides of 16S rRNA gene	Closely related validly published taxa	Sequence accession number of closely related species	Similarity %age of 16S rRNA gene sequence with closely related species	No. of closely related species having >97% (>98%) similarity of 16S rRNA gene sequence
1.	U7(1)	402	Staphylococcus epidermidis (NCTC 11047(T)	UHDF01000003	99.75	>30
2.	U6	981	Staphylococcus aureus subsp. aureus (DSM 20231T)	AMYL01000007	99.39	6(5)

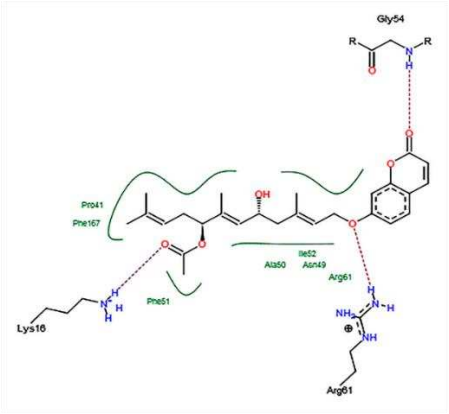

(**1**)

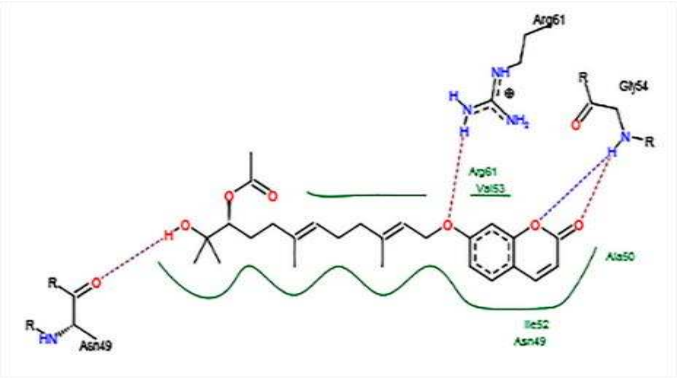

(**2**)

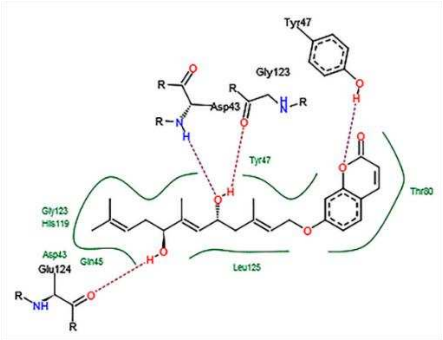

(**3**)

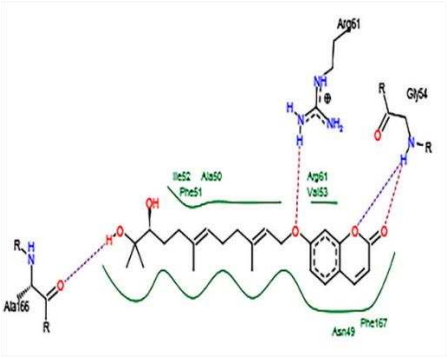

(**4**)

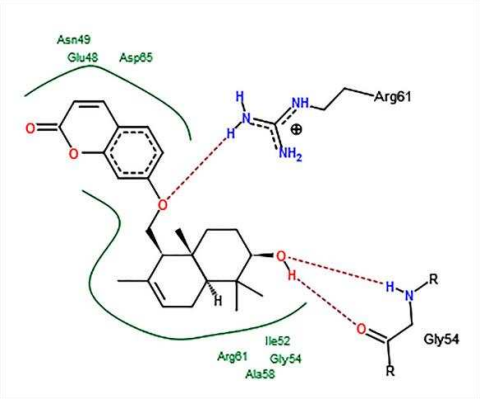

(**5**)

Figure S1. 2D interactions of **1**) 8'-O-acetyl-asacoumarin A **2**) 10' R-acetyl-karatavacinol **3**) Asacoumarin A; **4**) 10' R-karatavacinol **5**) Feselol inside the pocket of transcriptional regulator 2UV0 (dotted lines present hydrogen bonding while green complete lines show hydrophobic interactions)

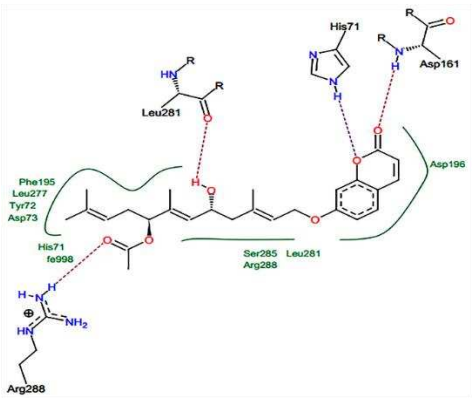

(**1**)

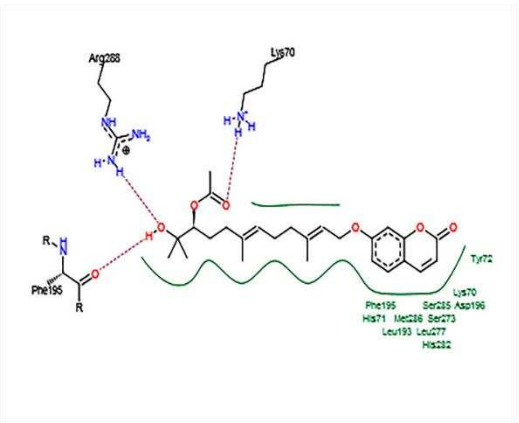

(**2**)

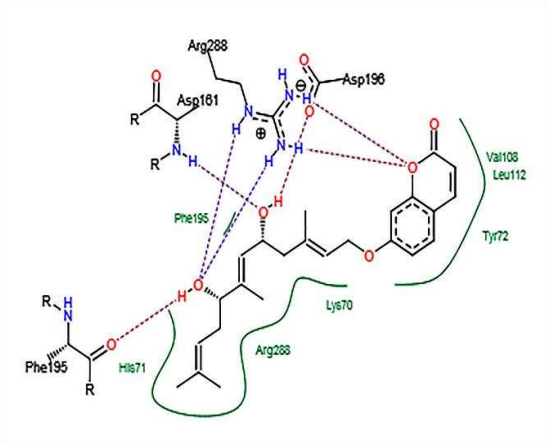

(**3**)

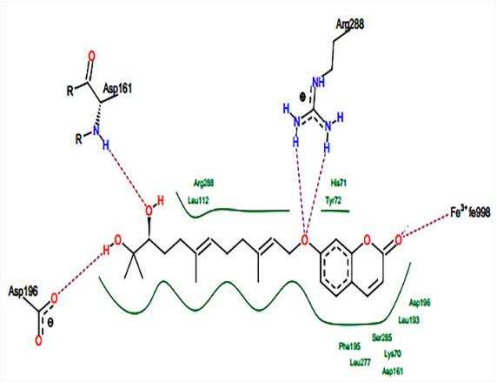

(**4**)

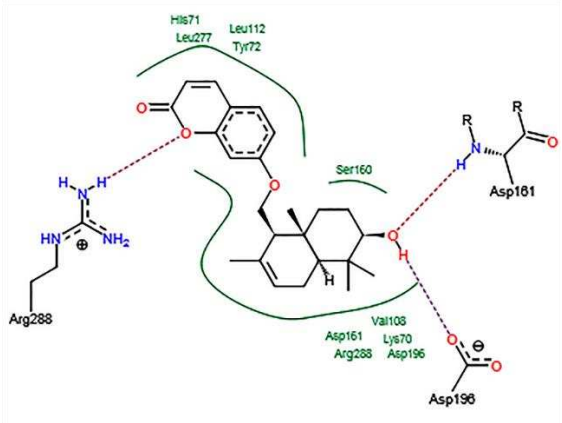

(**5**)

Figure S2. 2D interactions of **1**) 8'-O-acetyl-asacoumarin A **2**) 10' R-acetyl-karatavacinol **3**) Asacoumarin A; **4**) 10' R-karatavacinol **5**) Feselol inside the pocket of transcriptional regulator 2Q0J (dotted lines present hydrogen bonding while green complete lines show hydrophobic interactions)

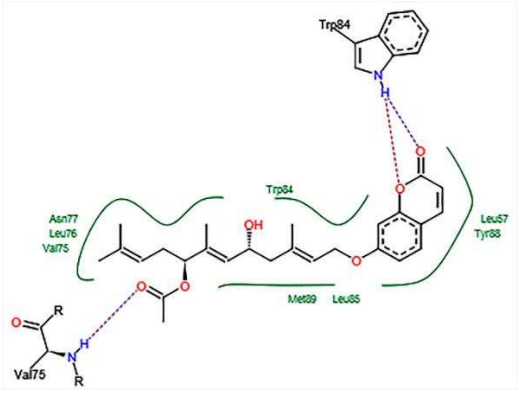

(**1**)

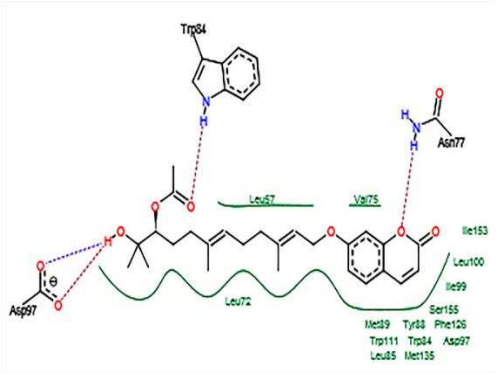

(**2**)

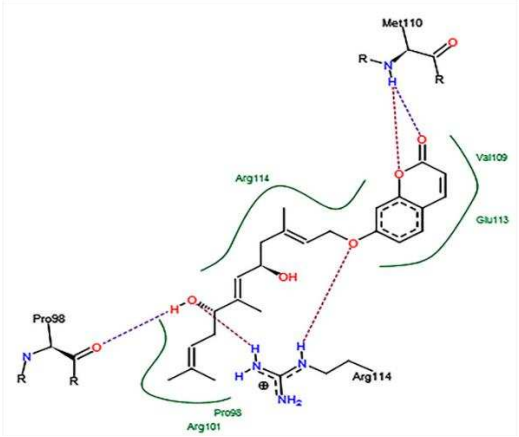

(**3**)

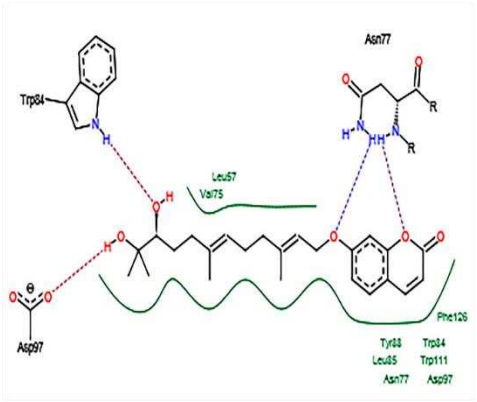

(**4**)

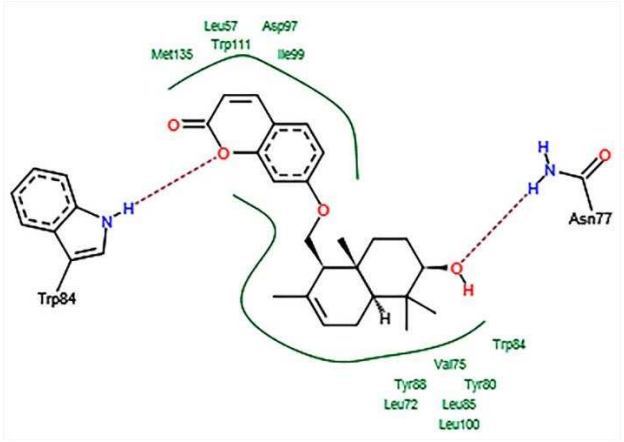

(**5**)

Figure S3. 2D interactions of **1**) 8'-O-acetyl-asacoumarin A **2**) 10' R-acetyl-karatavacinol **3**) Asacoumarin A; **4**) 10' R-karatavacinol **5**) Feselol inside the pocket of quorum sensing regulators CviR (3QP5) (dotted lines present hydrogen bonding while green complete lines show hydrophobic interactions)

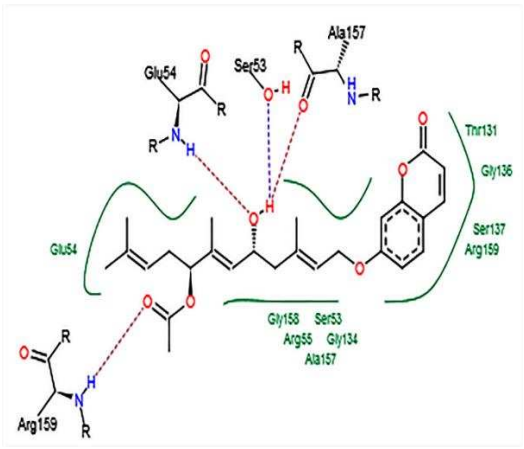

(**1**)

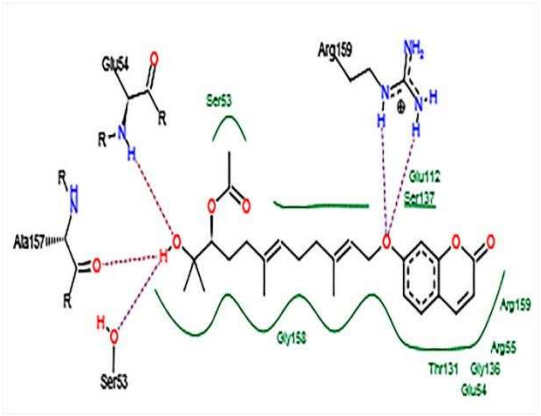

(**2**)

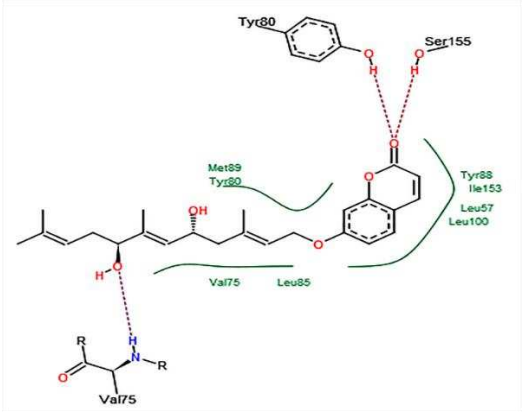

(**3**)

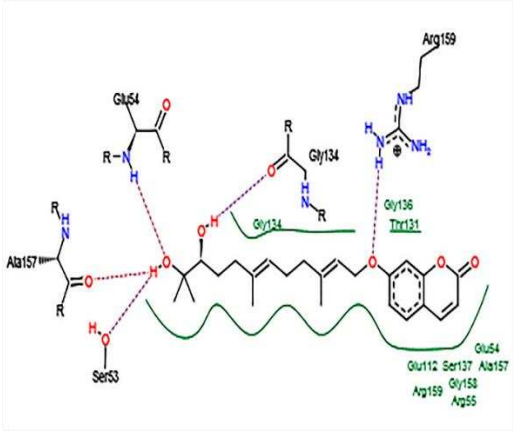

(**4**)

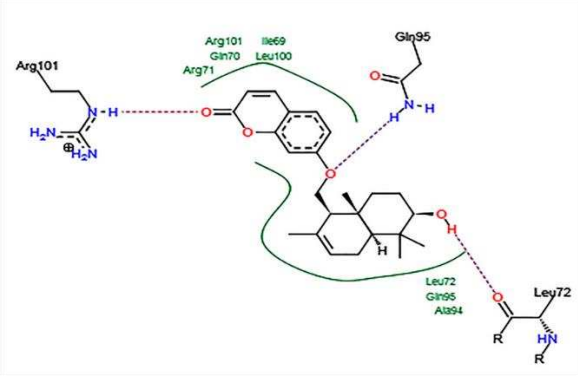

(**5**)

Figure S4. 2D interactions of **1**) 8'-O-acetyl-asacoumarin A **2**) 10' R-acetyl-karatavacinol **3**) Asacoumarin A; **4**) 10' R-karatavacinol **5**) Feselol inside the pocket of quorum sensing regulators CviR' (3QP1) (dotted lines present hydrogen bonding while green complete lines show hydrophobic interactions)